Key Words:

#Key1#
#Key2#

Retention:
#Permanent#

MINERALOGICAL AND MICROSTRUCTURAL EVOLUTION IN HYDRATING CEMENTITIOUS SYSTEMS

Kenneth A. Snyder

MARCH 31, 2009

Savannah River National Laboratory
Savannah River Nuclear Solutions
Aiken, SC 29808

Prepared for the U.S. Department of Energy Under Contract Number DE-AC09-08SR22470

TABLE OF CONTENTS

LIST OF FIGURES

LIST OF TABLES

LIST OF ACRONYMS

AAS	Alkali Activated Slag
ASTM	ASTM International
CBP	Cement Barriers Partnership
CEMHYD3D	CEMent HYDration model in 3-Dimensions
C-S-H	Calcium Silicate Hydrate gel (amorphous)
DLA	Diffusion Limited Aggregation
DOE	U.S. Department of Energy
GEMS	Gibbs Energy Minimization Selektor
GGBFS	Ground Granulated Blast Furnace Slag
MIP	Mercury Intrusion Porosimetry
PHREEQC	pH-REdox-EQuilibrium-C (programming language)
QXRD	Quantitative X-Ray Diffraction
SRS	Savannah River Site

ABSTRACT

The mineralogical and microstructural changes that occur in cementitious systems during hydration are summarized. These changes depend, in large part, on the proportions of the cementitous binders (portland cement, fly ash, silica fume, and slag). Moreover, these changes are discussed in the context of hydration under sealed (no chemical exchange with the environment) and iso-thermal conditions. Under these conditions, the hydration reactions, and commensurate mineralogical and microstructural changes, continue over the time scale of months or years. The few very slow reactions are discussed in the context of thermodynamic modeling.

The mineralogical and microstructural stability at very long time scales (e.g., centuries, millennia, etc.) is relevant to performance assessment for nuclear applications. The very long-term stability of the hydrated phases is discussed in the context of natural and ancient analogs.

Microstructural changes due to degradation are discussed in the general context of physico-chemical service life computer modeling; the mineralogical changes due to degradation are discussed in the chapter on chemical degradation. Because there are no analytical expressions for the microstructural changes that occur during degradation (besides changes in the porosity), computer models must rely on empirical expressions that are applied to all chemical degradation mechanisms simultaneously. As a result, the microstructural changes are discussed in the broad context of modeling, without reference to specific degradation mechanisms.

For relevance to nuclear applications, various cementitious systems are considered. These include systems having a broad range of proportions of cement, fly ash, slag, and silica fume. Moreover, the possible effects of waste stabilization, through incorporation into the mix water, are discussed.

1.0 INTRODUCTION

Cementitious barriers for nuclear applications must satisfy both mechanical and chemical performance criteria. A comprehensive performance assessment tool, as is being developed in the Cement Barriers Partnership (CBP) project, must be able to assess both types of performance. To do this, the tool must be able to quantify the chemical and physical properties of the mineralogy and the microstructure of the composite system (binder and aggregate). Moreover, the assessment tool must be able to predict changes in the mineralogy and the microstructure due to either continued hydration of the cementitious components, or due to the chemical reactions that are part of any number of degradation mechanisms.

Anticipating the mineralogical and microstructural changes that occur in cementitious systems, either due to hydration or due to degradation, is an important component of accurate performance prediction and assessment. The mineralogical makeup and microstructural transport properties determine the chemical stability of the solid, (in some cases) the mobility

of species, and the overall hydraulic flow through the system. Predicting these changes is relevant to the CBP technical challenges because a cementitious system is always hydrating, and (almost always) interacting with its environment. Moreover, in practical applications, hydration and degradation are occurring at the same time.

Predicting the mineralogical and microstructural changes during hydration alone is a difficult challenge. There is a wide range of possible blended cementitious mixtures that may be used in the nuclear infrastructure, and the specific physical/chemical properties of supplementary materials that influence hydration are not completely understood. The different components of a nuclear facility may require a range of mechanical, chemical, and physical properties. The optimal mixture for each element may require two or three cementitious materials.

Fortunately, hydration and degradation are both controlled by transport of ionic species in the aqueous pore solution and chemical reactions between ionic species in the pore solution and the soluble mineral phases present. In effect, hydration and degradation involve the same chemical and physical mechanisms; only the specifics differ. In effect, the mineralogical and microstructural changes due to hydration or degradation are part of a continuous spectrum.

Long-time modeling of cementitious systems consists of treating the material as a porous composite in equilibrium with the aqueous pore solution within the paste fraction of the cementitious composite. Upon enumerating all the relevant chemical reactions, a thermodynamic model can be used to calculate the mineral phase composition that is in equilibrium with the pore solution. These changes in the pore solution can occur through continued hydration (dissolution of the starting cementitious starting materials) or through interaction with the material's environment. The equilibrium calculation yields the quantity of mineral phases that must either dissolve or precipitate, thereby changing the porosity and the transport properties, which can be re-calculated by a 3-D microstructure model. By treating all degradation mechanisms in the same manner, multiple degradation mechanisms can be occurring simultaneously.

A key element to this approach is sufficient and accurate thermodynamic data for all the relevant chemical reactions (hydration and degradation). Data exist for nearly all the relevant reactions for portland cement, fly ash, ground granulated blast furnace slag, and silica fume. For some mineral phases, however, more accurate data are needed for the solubility and the temperature dependence, which may be an important issue for waste immobilization.

Another key element to the thermodynamic approach to mineralogical evolution is that kinetics are independent of thermodynamics. Although most of the reactions occur over the time scales of laboratory measurements, there are some reactions that occur over very long times, and may be important to the overall performance. These reactions involve either re-crystallization of hydrated phases, or the crystallization of the amorphous calcium silicate gel that constitutes the major phase of hydrated cementitious systems. The rates of these reactions are not known, and are important for long-term performance prediction.

1.1 PRESENT STATE OF HYDRATION MODELING

There exist two types of hydration models: microstructural models and thermodynamic models. The microstructural models like CEMHYD3D[1] (Bentz, 1997) and μic[2] (Scrivener & Bishnoi, 2009) attempt to predict details of the hydrated microstructure with the intent of predicting transport and mechanical properties. The thermodynamic models like GEMS[3] (Lothenbach & Winnefeld, 2006) use empirical kinetic models to predict the quantity of solid phases present, the porosity, the water content, and the pore solution composition as a function of time.

The microstructural models are not entirely physical, and the predicted transport coefficients (diffusivity and permeability) have not been validated to the extent necessary for reliable long-term performance prediction. Moreover, the chemistry incorporated into these models may not be consistent with existing thermodynamic data. On the other hand, the thermodynamic models neglect physical properties and microstructure evolution. Any attempt to couple microstructural and thermodynamic models together must overcome these issues.

In addition, a hydration model having practical relevance to the nuclear infrastructure will have to be applicable to a wide spectrum of cementitious component proportions. (Existing hydration models were developed primarily for predicting the hydrated phases of pure portland cement). Some hydration models can predict, to some degree, the hydration products of systems in which a relatively small to moderate fraction of the portland cement has been replaced by any one of fly ash, silica fume, or slag. Moreover, these models are limited to mixtures in which the 'mix water' is either distilled water or from the municipal water supply. Unfortunately, hydration models have not been validated for systems where portland cement comprises less than one-half of the cementitious components, or for mixtures prepared with concentrated salt solutions.[4]

2.0 MINERALOGY OF CALCIUM SILICATE CEMENT SYSTEMS AND HYDRATION PRODUCTS

The cementitious binders of practical concern include portland cement, fly ash, ground granulated blast furnace slag (GGBFS), and silica fume. Portland cement is largely crystalline, and the other binders are mostly glass. Each contributes to the calcium and/or silica contents required to form an amorphous calcium silicate hydrate (C-S-H) gel, the primary binding phase for all these systems. Portland cement and (sometimes) slag are the

[1] A pixel-based microstructural development tool that recreates paste microstructures (at a fixed 1 μm pixel size) consistent with SEM micrographs.
[2] Pronounced "mic", the model works with discrete (spherical) elements that have a location and size. Although the model achieves the correct volume fractions and has arbitrary spatial resolution, the resulting microstructures do not resemble micrographs of cement pastes.
[3] http://gems.web.psi.ch/
[4] Relatively limited engineering experience is available for most waste forms (Bradford et al. 2005).

only binders that contain sufficient lime and silica, and in the proper proportions, to produce a solid hydrated mass upon mixing with water. Some Class C fly ashes also have this characteristic and are referred to as hydraulic fly ashes.

Typical oxide contents of portland cement, fly ash, blast furnace slag, and silica fume are shown schematically in Figure **1**. Because cementitious materials are also composed of other oxides, Figure **1** represents the typical ranges of CaO, SiO_2, and Al_2O_3 present in these materials.

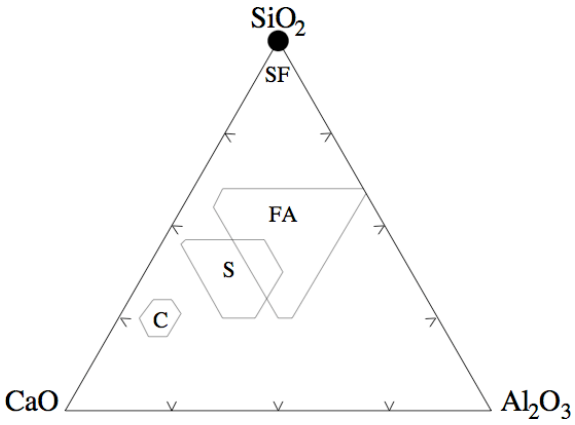

Figure 1. Approximate range of oxide contents for cement (C) fly ash (FA), blast furnace slag (S), and silica fume (SF). (Smolczyk 1980, Mindess & Young 1981, Uchikawa 1986)

Industry practice for characterizing a cementitious binder is most often limited to the oxide content of the binder. The oxide content alone, however, is insufficient for determining the reactivity of the binders. Additional characterization of the material is needed to determine the type and quantity of crystalline and glassy mineral phases present. Unfortunately, the crystalline binder (portland cement) and glassy binders (fly ash, silica fume, and GGBFS) require different techniques to determine the reactivity of the material.

2.1 PORTLAND CEMENT AND CEMENT HYDRATION PRODUCTS

Historically, cement chemistry researchers have developed a shorthand notation for the oxides commonly found in portland cement, and the notation proves useful in characterizing the other cementitious materials as well. The shorthand is summarized in Table 1.

Table 1. Cement chemistry notation for oxides related to portland cement.

Oxide Composition	Cement Chemistry Notation
CaO	C
SiO_2	S
Al_2O_3	A

Fe_2O_3	F
SO_3	$\overline{S}$
CO_2	$\overline{C}$
K_2O	K
Na_2O	N
MgO	M
H_2O	H

The mineral composition of portland cement is most often estimated from the cement oxide contents. This 'Bogue calculation' (Bogue 1929) is a mathematical means of de-convolving the oxide components into an estimated mineral phase composition. ASTM C 150 (ASTM 2005a) has implemented an extended version of the original Bogue calculation that assumes cement is composed of six pure phases (C_3S, C_2S, C_3A, C_4AF, $C\overline{S}$, $C\overline{C}$). Another technique developed by Taylor (Taylor 1997) includes additional alkali sulfate phases and assumes that certain mineral phases contain impurities.

Quantitative X-ray diffraction (QXRD) using Rietveld analysis has been used to demonstrate that these calculations are unreliable and inaccurate, especially for minor mineral phases (Stutzman 2008). Because of the discrepancy between calculated and measured mineral phases, QXRD is the only reliable means (presently) for determining the mineral phase content of portland cement. The procedure is outlined in ASTM C 1365 (ASTM 2006b).

A summary of mineral phase mass fractions typically found in portland cement (Mindess & Young 1981) is given in Table 2 merely as a frame of reference for the reader. The mass fractions given in Table 2 represent an average, do not necessarily represent any particular cement, and are based on the Bogue calculation. These values are meant to demonstrate the type of variability expected among the different types of cement.

Table 2. Typical mass fractions of mineral phases found in commercial ASTM portland cement types. (Mindess & Young 1981)

	Typical Mass Fractions				
Phase	**Type I**	**Type II**	**Type III**	**Type IV**	**Type V**
C_3S	0.50	0.45	0.60	0.25	0.40
C_2S	0.25	0.30	0.15	0.50	0.40
C_3A	0.12	0.07	0.10	0.05	0.04
C_4AF	0.08	0.12	0.08	0.12	0.10
$C\overline{S}H_2$	0.05	0.05	0.05	0.04	0.04

As can be seen in Table 1, portland cements are largely composed of alite (C_3S) and belite (C_2S), each containing impurities such as alkalis. Gypsum ($C\overline{S}H_2$) is added at the time of grinding; it is also common for portland cement producers to add small quantities (5 % maximum) of limestone ($C\overline{C}$) along with the gypsum. The C_4AF phase represents one

particular point in the series of possible ferrites phases with composition $Ca_2(Al_xFe_{1-x})_2O_5$, where $0 < x < 0.7$ (Taylor 1997).

Assuming that each phase in Table 2 is pure, the corresponding oxide contents are given in Table 3. The C/S mass ratio for most portland cements is approximately 3:1, and the C/A mass ratio varies from 10:1 to 15:1, depending upon the cement type.

Table 3. Typical mass fractions of oxides found in commercial portland cements, based on data in Table 2. (Mindess & Young 1981)

	Typical Mass Fractions				
Oxide	**Type I**	**Type II**	**Type III**	**Type IV**	**Type V**
C	0.663	0.647	0.660	0.613	0.643
S	0.219	0.223	0.210	0.240	0.245
A	0.062	0.052	0.054	0.044	0.036
F	0.026	0.039	0.026	0.039	0.033
$\overline{S}$	0.029	0.029	0.029	0.023	0.024

2.1.1 Alite and Belite Hydrated Phases

Alite (C_3S) and Belite (C_2S) react with water to form approximately equal parts (molar basis) portlandite (CH) and an amorphous calcium silicate hydrate gel (C-S-H gel); the hyphens denote a non-stoichiometric mixture. The Ca/Si molar ratio within C-S-H derived from alite and belite hydration typically varies over the range 1.6 to 2.0 (Taylor 1997).

The C-S-H gel is not a pure calcium silicate. The C-S-H may contain both metal ions and alkali ions as impurities (Taylor 1987). The amount of alkali binding depends upon the Ca/Si molar ratio in the C-S-H and the extent of aluminum substitution for silicon (Hong and Glasser 1999, 2002, Brouwers and van Eijk 2003). The extent of alkali binding has a significant effect on the pore solution pH.

In the absence of other hydrating minerals, CH and C-S-H are stable for very long times under sealed isothermal conditions. In the presence of pozzolanic silica-rich binders (e.g., fly ash, silica fume, etc.), however, the CH may be react to form additional C-S-H gel.

2.1.2 Aluminate, Ferrite, and Sulfate Hydrated Phases

Hydration of aluminate and ferrite phases most often leads to the formation of either AFm[5] phases or AFt[6] phases. The ratio of AFm to AFt formed will depend upon the amount of available alumina and sulfur.

[5] AFm (Al_2O_3-Fe_2O_3-*mono* CaX) phases are characterized by the chemical composition $C_3(A,F)\cdot CX\cdot yH$ where X represents a divalent anion typical for cement hydration, such as, $2OH$, $2Cl^-$, SO_4^{2-}, or CO_3^{2-}.

[6] AFt (Al_2O_3-Fe_2O_3-*tri* CaX) phases are characterized by the chemical composition $C_3(A,F)\cdot 3X\cdot yH$ where X again represents a divalent anion typical for cement hydration.

The numerous AFm phases that can be created during portland cement hydration have the following chemical form $C_4(A,F)X \cdot yH$. Under ideal conditions, AFm phases typically form platey, hexagonal crystals (Taylor 1997). Most of the AFm phases produced through portland cement hydration, however, are poorly crystalline and interspersed within the C-S-H phase (Taylor 1997). Monosulfate ($C_3A \cdot C\overline{S} \cdot 12H$) is an AFm phase often associated with sulfate attack.

The stability of monosulfate increases with increasing temperature, and forms at elevated temperatures (Matschei et al. 2007). In addition, monosulfate can react with CO_3^{2-} in presence of CH to form ettringite and hemicarbonate (Taylor 1997), which is relevant to modern cements that may contain limestone.

AFt phases are typically hexagonal prismatic or acicular crystals (Taylor 1997). In contrast to AFm phases, there are only two AFt phases significant to portland cement hydration: ettringite ($C_3A \cdot 3C\overline{S} \cdot 32H$) and thaumasite ($C_3S \cdot \overline{C}\overline{S} \cdot 15H$). Ettringite is an expansive reaction product (with respect to monosulfate) that typically occurs through sulfate attack by the conversion of monosulfate in the presence of excess calcium and sulfate. Thaumasite is thought to form from one (or more) of three possible mechanisms (Crammond 2003): 1) a topochemical interchange of ionic species; 2) precipitation in solution; and 3) nucleation using ettringite as a template. Little is known of the reaction path, and even less is known of the reaction kinetics.

2.1.3 Siliceous Hydrogarnet Phases

The term 'hydrogarnet' is typically defined in the literature as a calcium aluminate hydrate: $Ca_3Al_2(OH)_{12}$. The presence of silica species in the pore solution of cementitious materials leads to the formation of siliceous hydrogarnets. The hydrogarnet phases are cubic and form solid solutions with end members being grossularite ($Ca_3Al_2Si_3O_{12}$) and katoite ($Ca_3Al_2(OH)_{12}$). Intermediate phases are formed by F replacing A, and H replacing S. These phases have the generalized chemical formula $C_3A_xF_{1-x}S_nH_{6-2n}$ where $0 \le x \le 1$ and $n = \{0,1,2,3\}$. Of the ternary system $CaO - Al_2O_3 - H_2O$, only C_3AH_6 is stable at ordinary temperatures (Taylor 1997). The other phases are more common in autoclaved cementitious systems or as a hydration product of calcium aluminate cements.

These phases are rather complicated, and require further research. Laboratory synthesis of intermediate siliceous hydrogarnet phases typically yielded distinct phases, indicating a miscibility gap (Jappy and Glasser 1991), or contained irreducible quantities of C-S-H (Matschei et al. 2007), adding uncertainty to the estimated thermodynamic parameters. Silicious hydrogarnet phases are thought to be the stable state of AFm, but the kinetics are unknown. More research is needed for very long-term performance prediction.

2.1.4 Hydrated Magnesium Phases

Hydrated magnesium phases can occur when the cement has a relatively large magnesium content. The most common hydrated phases are brucite (MH) and hydrotalcite ($M_4A\overline{C}H_8$). Another common form of hydrotalcite occurs when OH^- replaces CO_3^{-2} to yield M_4AH_{10} (meixnerite). The reactivity of periclase (MgO) is relatively unknown, and it can remain unreacted in the paste for months.

2.1.5 Proportions of Portland Cement Hydrated Phases

Typical mass fractions of reaction products in hydrated 0.50 water:cement mass ratio portland cement paste are given in **Error! Reference source not found.** (Lothenbach & Winnefeld 2006). C-S-H constitutes the majority of the hydration product, followed by (roughly) equal proportions of portlandite, monocarbonate, and ettringite. Because magnesium is a minor component in portland cement, hydrotalcite is a minority hydrated phase.

Table 4. Representative hydrated phase mass fraction for a 0.50 water:cement (mass) ratio portland cement paste (Lothenbach & Winnefeld 2006).

Phase	Mass Fraction
C-S-H	0.45
CH	0.20
Monocarbonate	0.15
Ettringite	0.13
Hydrotalcite	0.04

2.2 SLAG CEMENT

Slag can react on its own if the pH is kept sufficiently high through the use of an activator such as calcium hydroxide, sodium hydroxide, or sodium silicate (Yuan & Xin 1992, Taylor 1997). For these alkali activated slags (AAS), the accelerator is typically 3.5 % to 5.0 % (by mass) Na_2O added as NaOH or sodium silicate. Calcium sulfate can accelerate the reaction by precipitation of ettringite to provide a sink for Ca^{2+} and $Al(OH)_4^-$ ions released from slag, but additional alkali must be present (Regourd 1980).

The primary hydration products of AAS are C-S-H, hydrotalcite, and AFm (Jiang et al. 1997, Wang & Scrivener 2005, Gruskovnjak et al. 2006). The Ca/Si ratio in the C-S-H formed from AAS is typically 1.1-1.2, which is low in comparison with hydrated portland cement.

Supersulfated cements consist (mass percent) of 80 % to 85 % slag, 10 % to 15 % anhydrite, and approximately 5 % activator that is usually portland cement clinker, and is ground more finely than ordinary portland cements. (Taylor 1997) The main reaction products are C-S-H

and ettringite (Taylor 1997) with minor constituents hydrotalcite, gypsum, and merwinite (C_3MS_2) (Gruskovnjak 2008).

2.3 BINARY BLENDED CEMENT SYSTEMS

In many engineering applications, the most desirable properties are achieved by using binary mixtures of portland cement and a supplemental mineral admixture such as fly ash, slag, or silica fume. Each mineral admixture has unique qualities for particular applications. In virtually all cases, mixtures are designed such that the supplemental mineral admixture replaces some portion of the portland cement.

One common reason for adding supplemental pozzolans to portland cement mixtures is to consume the portlandite from portland cement hydration. The supplemental materials are typically composed of considerably more silica than calcium (silica-rich). The silica reacts with available portlandite to form additional C-S-H gel. Because the C-S-H is far more stable than portlandite, eliminating portlandite from the final hydration products could have a dramatic impact on the long-term leaching characteristics and on the pore solution pH of the system.

2.3.1 Portland Cement – Fly Ash

There are two commonly used classes of fly ash: Class C and Class F. The ASTM C 618 (ASTM 2005b) limits for the oxides present in Class F and Class C fly ash are given in Table 5. Class C fly ashes, by virtue of having less silica, alumina, and ferrite, have more calcium than Class F fly ashes.

Table 5. Oxide requirements for ASTM C 618 Class F and Class C fly ash (ASTM 2005b).

	Class F	Class C
S+A+F	> 70 %	> 50 %
$\overline{S}$	< 5 %	< 5 %

Some Class C fly ashes are able to set and harden when mixed with only water, and are thus true hydraulic cements (Taylor 1997). The use of these stand-alone fly ash mixtures, however, is rare. When used, the initial hydration products include ettringite (Solem & McCarthy 1992).

The vast majority of both Class F and Class C fly ash is a glassy mixture of calcium, silicon, and aluminum oxides. The glassy phases in Class F fly ashes are higher in SiO_2, and the crystalline phases are typically mullite, quartz, magnetite, and hematite. The glassy phases in Class C fly ashes are higher in CaO, and the crystalline phases are typically quartz, lime, and periclase (Taylor 1997). The specifics of the elemental composition of the various glassy phases and the quantity and type of crystalline phases impact the fly ash reactivity, but little

is known of the significance of fly ash morphology on the final distribution of the mineral phases in hydrated cementitious systems.

As with most supplemental pozzolanic materials, the primary impact of fly ash replacement of cement is the reduction in the amount of portlandite produced and the reduced Ca/Si molar ratio in the C-S-H, typically near 1.5 initially and falling to 1.1 to 1.2 after 10 years (Taylor 1997). The hydration products of mixtures containing fly ash are very similar to the hydration products of pure portland cement pastes. The ratio of C-S-H to portlandite will increase, with the proportion of portlandite going to zero given sufficient fly ash replacement of cement.

The other types of crystalline hydrated phases are similar to those for pure portland cement paste. Within increasing fly ash content, the mass fraction of ettringite decreases due to cement sulfate dilution. The displacement of Portland cement also decreases the portland cement phase reactivity, so the mass fraction of unhydrated cement increases with increasing fly ash content. Some of the fly ash crystalline phases, notably quartz, can remain in the hydrated system for months because of the relatively low reactivity.

2.3.2 Portland Cement – Slag Cement

Blast furnace slag is a by-product of iron manufacturing when limestone reacts with SiO_2 and Al_2O_3 at very high temperatures. If forced to cool quickly below 800 ^oC, the result is a hydraulic cement that is over 95 % glassy. The glassy material is ground, yielding a ground granulated blast furnace slag (GGBFS) (Taylor 1997).

Typical GGBFS is glassy, with the following composition range: C: 30 % to 50 %; S: 27% to 42 %; A: 5 % to 33 %; and M: 0 % to 21 % (Smolczyk 1980). The crystalline phases in GGBFS, if present, are melilite $(Ca,Na)_2(Al,Mg,Fe^{2+})[(Al,Si)SiO_7]$ (sorosilicate: Si_2O_7) and merwinite $Ca_3Mg(SiO_4)_2$ (neosilicate) (Regourd 1986). The chemical requirements of slag conforming to ASTM C 989 (ASTM 2006a) are that the total sulfide (S^{2-}) be less than 2.5 %, and that sulfate reported as SO_3 be less than 4.0 %.

Slag is desirable for use in certain radionuclide applications because the sulfide content helps to provide a reducing environment within the pore space. In certain applications, such as the chemical stabilization of Tc-99, the mobility depends strongly on the reduction-oxidation (redox) potential within the pore solution.

The principal hydration products are similar to those from portland cement hydration. The most noticeable difference is the lower amount of CH produced, as compared with portland cement hydration. For 50 % cement replacement, the Ca/Si ratio was near 1.5 (Richardson & Groves 1992). Otherwise, the effect of slag on the hydrated phase mineralogy is very similar to that of fly ash.

2.3.3 Portland Cement - Silica Fume

Silica fume is a by-product of the industrial processes for making either silicon or silicon alloys, and the typical dispersed particle size is 100 nm. In industrial applications, the silica fume is often agglomerated and thus can have a much larger apparent particle size. The material is almost entirely glassy, and the most common crystalline impurities are KCl, quartz, metallic iron, and iron silicide (Taylor 1997). The ASTM C 1240 (ASTM 2005c) specification requires that the SiO_2 content of the silica fume be greater than 85 %.

Silica fume is most often added as a supplemental mineral admixture to accelerate hydration at early ages and to consume portlandite produced by portland cement hydration. At a cement replacement of 30 % (relatively high from a practical mix design stand point), the silica fume consumes all available CH by 14 d (Huang & Feldman1985a, 1985b). Another effect of silica fume as a replacement for portland cement is to reduce the Ca/Si molar ratio in C-S-H gel down to levels as low as 1.1 (Traetteberg 1978). The lower Ca/Si molar ratio C-S-H typically bind more Na and K, and also have more aluminum substitution for Si, resulting in higher effective surface charges.

2.4 TERNARY CEMENTITIOUS SYSTEMS

Although ternary mixtures are used in practice, these mixtures are typically composed of large percentages of portland cement and considerably smaller percentages of mineral admixtures. These ternary blends are used for specialty applications such as reducing susceptibility to alkali-silica reaction (Shehata & Thomas 2002). When used with large portions of portland cement, the (typical) effects of these ternary blends is to consume portlandite from the portland cement hydration reaction and to reduce the Ca/Si molar ratio of the C-S-H gel.

Other examples of termary binder systems are found in waste forms. The proposed Savannah River Site (SRS) saltstone waste form and similar salt waste forms proposed for Hanford are approximated by a 6:47:47 (mass ratio) mixture of cement:slag:fly ash (Bradford et al. 2005). The slag is added to help provide a reducing environment; the fly ash also contributes to a reducing environment, but to a less extent.

Work is needed to transfer existing engineering knowledge into present hydration models for such material systems. The primary difficulty lies in estimating the reactivity of the individual cementitious components, particularly for systems having very low cement content. Although thermodynamic models could be used today, the reactivity of the individual components would have to be estimated from laboratory experiments performed on the systems of interest.

The types of hydrated phases found in low-cement grouts made with portland cement, fly ash, slag, and distilled water are very similar to those for pure portland cement paste and binary mixtures. As for binary systems, the portlandite will be consumed, but at a much greater rate. Upon consumption of the portlandite, one may find strätlingite.

2.5 HYDRATION AT ELEVATED TEMPERATURES

Conditions may arise where the cementitious binder will hydrate under elevated temperatures; these conditions are considered separately from autoclaved conditions. In pastes cured at elevated temperatures, X-ray microanalysis suggests that the Ca/Si ratio increases as the temperature increases (Scrivener & Taylor 1993). But this may be due, in part, to incorporation of poorly crystalline portlandite into the C-S-H. As for ordered C-S-H at elevated temperatures, XRD gives no evidence of C-S-H crystallization at temperatures up to at least 100 °C (Taylor 1997).

When samples are exposed to elevated temperatures under saturated conditions for one year, ettringite begins to disappear above 70 °C, and is completely gone above 100 °C, unless there is excess aluminum, calcium and sulfate available (Buck et al. 1985). Moreover, above 100 °C, the ettringite was replaced by hydrogarnet, not monosulfate (Buck et al. 1985).

In another experiment, samples were first cured at 20 °C for 30 days, then cured at 85 °C for 8.4 years, and then returned to 20 °C for periods ranging from 1.5 years to 2.0 years; companion samples were cured at 20 °C for the entire 10 years (Paul & Glasser 2001). The samples cured at 25 °C were nearly completely hydrated, and the systems were composed primarily of C-S-H gel, portlandite, ettringite, and AFm. The samples cured at 85 °C showed no indication of additional hydration after the initial 20 °C curing period.

3.0 PORE SOLUTION COMPOSITIONAL EVOLUTION

The composition of the pore solution is estimated by determining the aqueous solution that is in equilibrium with the soluble mineral phases present. Because the pore structure of hydrated pastes is finely divided, the pore solution comes into contact with all mineral phases present. Moreover, because transport occurs at relatively long time scales, and reactions happen on relatively short time scales, the equilibrium assumption is reasonable. Similarly, changes in the pore solution composition, due to transport, may lead to dissolution/precipitation reactions that can change the microstructure and the transport properties.

Having an estimate for the pore solution composition can be important because sometimes the purpose of performance modeling is to estimate the chemical composition of the effluent from the cementitious structure. In these cases, accurate characterization of the pore solution can be vital to reliable performance assessment because the chemical composition of the effluent can have a significant impact on the overall performance.

The composition of the paste pore solution is determined experimentally by physical extraction. During the first few hours of hydration, the pore solution can be extracted by vacuum filtration or centrifuge (Gartner et al. 1985, Michaux et al 1989, Goldschmidt 1982).

At later ages, a high pressure press (Longuet et al. 1973, Barneyback & Diamond 1981) is needed to obtain a sufficiently large sample for analysis.

3.1 PORTLAND CEMENT PASTE PORE SOLUTION

The pore solution of typical cementitious mixtures is composed of a large number of ionic species. As an example, a portland cement mixture was characterized (Lothenbach & Winnefeld 2006) by the oxides present in the cement (see Table 6), and the elemental components of the pore solution (see Table 7); undoubtedly, there were other elements present in the pore solution, such as magnesium. The data in Table 7 suggest that the pore solution becomes stable between 100 d and 300 d hydration, before degradation begins.

Table 6. Cement oxide mass fractions from (Lothenbach & Winnefeld 2006).

Oxide Mass Fractions								
CaO	SiO_2	Al_2O_3	Fe_2O_3	SO_3	K_2O	Na_2O	MgO	CO_2
0.6320	0.1970	0.0470	0.0267	0.0335	0.0112	0.0008	0.0185	0.0193

Table 7. Pore solution composition (mmol/kg) from (Lothenbach & Winnefeld 2006).

Day	OH^-	K	Na	S(VI)	Ca	Si	Al
29	540	560	63	11	1.2	0.27	0.12
105	570	650	57	17	1.5	0.21	0.04
317	590	640	65	16	1.5	0.21	0.11

Using the PHREEQC (Parkhurst & Appelo 1999) speciation and thermodynamic equilibirum computer code, the component compositions in Table 7 were used to estimate the ionic species present, and the results are shown in Table 8; the boldface numbers represent the total quantity of the component.

Table 8. Speciation of the pore solution composition shown in Table 7, calculated using PHREEQC (Parkhurst & Appelo 1999).

Component	Species	mol/kg
	OH^-	0.613
K		**0.640**
	K^+	0.584
	KOH^o	0.050
	KSO_4^-	0.006
Na		**0.065**
	Na^+	0.055
	$NaOH^o$	0.010
S(VI)		**0.016**
	SO_4^{-2}	0.010

	KSO_4^-	0.006
Ca		**0.000480**
	$CaOH^+$	0.000308
	Ca^{+2}	0.000127
	$CaH_2SiO_4^o$	0.000033
	$CaSO_4^o$	0.000012
Si		**0.000154**
	$H_2SiO_4^{-2}$	0.000102
	$CaH_2SiO_4^o$	0.000033
	$H_3SiO_4^-$	0.000019
Al		**0.000110**
	$Al(OH)_4^-$	0.000110

The important thing to notice from the speciation calculation results in Table 8 is that each element was represented by two or more ionic species in the pore solution. Therefore, each component of a multidisciplinary degradation model has to determine which of the numerous ionic species present are important, and how best to represent the total component by ionic species.

3.2 BLENDED CEMENT MIXTURES

The primary difference between the pore solution of blended cement systems and pure portland cement systems is the pH. This is due to both the alkali sorption of the lower Ca/Si ratio C-S-H and the consumption of portlandite by the silica-rich supplemental cementitious materials. In general, fly ash, slag, and silica fume do not contribute new components to the pore solution. The only notable exception is titanium in fly ash.

3.3 SALTSTONE

The Department of Energy (DOE) developed a low-activity waste form, "saltstone," that is a grout composed of a salt waste solution that is blended with cement, slag, and fly ash. The fresh grout is pumped into engineered disposal vaults where it solidifies (Bradford et al. 2005). Although the possible cementitious mixtures can vary, one recommended composition is given in Table 9 (Cook & Fowler 1992, Cook et al. 2005). The grouts contain of very little portland cement to reduce the heat of hydration, and slag for the sulfite content that help to keep the pore solution in a reduced state.

Table 9. Proposed saltstone composition (Cook & Fowler 1992, Cook et al. 2005).

Component	Mass Fraction
Waste Salt Solution (29 % solids)	0.47
Slag: Grade 120	0.25
Fly Ash: Class F	0.25
Portland Cement: ASTM Type II	0.03

For saltstone waste forms and other spent acid-base waste streams, the 'mix water' is typically a highly concentrated aqueous solution of inorganic and/or organic species. The composition of a simulated salt waste stream stabilized in a hydroceramic material is provided in Table 10 (Bao, Grutzeck & Jantzen 2005). The solution is highly concentrated (29 % solids), and an analysis using the PHREEQC code indicates that the pH is nearly 14, and the activity of water is approximately 0.86.

Table 10. Example of simulated low-activity waste composition used to prepare hydroceramic waste forms (Bao, Grutzeck & Jantzen 2005).

Compound	g/L	mol/L
NaOH	105.9035	2.6478
$NaNO_3$	155.6883	1.8317
Na_2CO_3	123.0559	1.1610
$NaNO_2$	69.0892	1.0014
$Al(NO_3)_3 \cdot 9H_2O$	121.1723	0.3230
NaF	5.5596	0.1324
Na_2SO_4	11.7463	0.0827
NaCl	2.2999	0.0394
$Fe(NO_3)_3 \cdot 9H_2O$	15.0138	0.0372
KOH	2.0483	0.0365
Na_2HPO_4	4.0852	0.0288
$Ca(NO_3)_2 \cdot 4H_2O$	2.5171	0.0107
NiO	0.4537	0.0061
$Na_2Cr_2O_7 \cdot 2H_2O$	0.6532	0.0022
PbO	0.3172	0.0014
La_2O	0.0307	0.0001
$CsNO_3$	0.0157	0.0001

The alkalis and heavy metals may remain in the pore solution, may combine with other species to form mineral phases, or may be incorporated as an impurity in other hydrated phases. Determining the fate of these species requires incorporating the appropriate mineral phases into the chemical equilibrium calculation, and also having a reliable model for binding.

Under the right conditions, the mineral phases produced by these systems will differ from typical portland cement mixtures. Low calcium mixtures of ASTM Class F fly ash and clay with alkaline mix water at elevated temperatures may form zeolites (Brough et al. 1995, Katz et al. 2000). To address this in performance assessment tools, data for zeolites need to be added to the thermodynamic databases for cementitious systems.

3.4 LONG-TERM C-S-H STABILITY

The primary hydration product of portland cement-based systems is an amorphous C-S-H gel. Amorphous materials generally have greater free energies of formation than crystalline materials with similar elemental composition. Therefore, over very long time scales, one expects amorphous materials to slowly convert to crystalline materials. This expectation and the lack of experimental data spanning millenia have limited the acceptance of cement-based materials for use in very long time (centuries to millenia) waste isolation.

If future experiments can demonstrate the conversion/re-crystallization process for C-S-H, and the conditions under which the conversion occurs, one could use this evidence to predict very long-term performance. Given the limited set of elemental components present in cement-based materials, a conversion process will most likely result in the formation of familiar compounds. This information could be used to predict the chemical performance of the system over very long times; the mechanical properties may be much more difficult, or nearly impossible, to predict.

3.4.1 Natural/Ancient Analogs

Studying ancient binders and natural analogs is one approach to predicting the very long-term performance cement-based barriers. Although material formulation technology has changed since ancient times, the constituents of concretes made with ancient cements consist of hydrated calcium silicates, ettringite, etc. (Petit 1992).

There have been reports made on the properties of old cements (Steadman 1986) and archaeological binders (Jull and Lees 1990). Although direct comparisons to modern cements are problematic, the hydrated phases found in ancient, old, and modern cement-based binders are similar. This is particularly true for binders made from fired clays and volcanic rocks that contain silicon and aluminum. In these cases, the silicates, silica-aluminates, and aluminates bear a resemblance to the hydration products from modern cements (Petit 1992).

Studies of C-S-H from samples over 1800 years old suggest that the C-S-H is more stable than originally thought. Given the amorphous nature of C-S-H, the prevailing theory was that this material would, over long times, organize into a collection of related crystalline minerals such as tobermorite, jennite, and portlandite. The absence of this conversion in ancient cementititous systems suggests that the kinetics of any C-S-H crystallization is extremely slow. Moreover, the data suggest that systems with a lower Ca/Si molar ratio seem to have a greater C-S-H stability (Petit 1992).

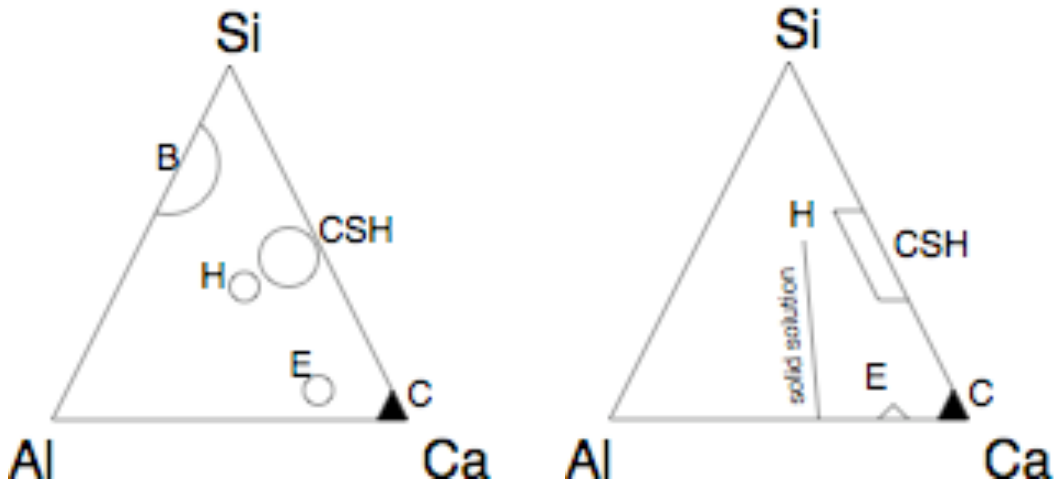

Figure 2. Ternary composition of Gallo-Roman binders (l) and modern pozzolanic cement (r) from (Rassineux et al. 1989): B: brick; H: silicious hydrogarnet; E: ettringite; C: calcite.

There are no published data to indicate the existence of C-S-H compounds in ancient binders (Rassineux et al. 1989). Instead, authors have concluded that these ancient binders were solely composed of calcite (see references in Rassineux et al. 1989). A more careful mineralogical study of Gallo-Roman binders revealed a material resembling C-S-H having a Ca/Si molar ratio varying from 1.0 to 1.2, and containing up to 5 % (by mass) Al_2O_3, up to 2 % (by mass) MgO, and up to 0.5 % (by mass) Fe_2O_3 (Rassineux et al. 1989). A more detailed characterization of the phases is shown in Figure 2 for both the ancient binders and more modern binders.

There exist rock formations, primarily limestones with clay and/or manganese impurities (Bogue 1955), that contain quantities of calcium, silicon, and aluminum in roughly the same proportions as portland cement. Upon calcining, these 'natural cements' are hydraulic, and their properties have been reported upon since the eighteenth century (see Bogue 1955).

The utility of studying existing examples of these materials may be more for the general behavior than any specifics. The starting materials would be poorly characterized by today's standards. Moreover, there would be very little similarity to modern portland cement. Furthermore, an analysis of phases found in existing examples would have to disentangle effects due to hydration and effects due to exposure.

The more general utility of existing examples of natural/ancient analogs may be in the detection of crystalline calcium silicate hydrates. The existence of crystalline calcium silicate hydrates having Ca/Si molar ratios similar to those found today (0.9 to 1.8) may give some insight into the rate of crystallization of amorphous calcium silicate gels. This type of information may be beneficial to very long-term studies of cementititous materials performance.

4.0 MICROSTRUCTURAL EVOLUTION

Modeling the state of a cementitious material, whether in a closed system or one exposed to degradation mechanisms, requires modeling transport and reaction through the hydrated cementitious binder. The physico-chemical approach to hydration and degradation modeling uses the environment as a boundary condition, allows transport to occur through the pore space, and calculates the thermodynamic equilibrium (or appropriate kinetic approach) distribution of components between the mineral phases and the pore solution species. The change in the mineral phases is determined by the chemical state of the system and the thermodynamic data. The change in the microstructure is due to dissolution and/or precipitation of mineral phases, which changes the porosity. The pore space tortuosity, however, is also changed and needs a 3-D microstructure model to properly compute the new transport coefficients.

The advantage of a physico-chemical approach is the ability to accommodate multiple simultaneous degradation mechanisms. All the degradation mechanisms are treated the same. The accuracy by which a degradation model accounts for a specific degradation mechanism is limited by the quality of the thermodynamic data for the anticipated reactions. Furthermore, transport through the system can be described by a number of material parameters and transport coefficients (e.g.: porosity, tortuosity, permeability, hydraulic diffusivity, etc.). Therefore, to model hydration and degradation, one needs to know how changes in the microstructure affect each of the material parameters and transport coefficients.

4.1 CHEMICAL REACTION

The key to successful physico-chemical modeling is accurate thermodynamic data for the relevant mineral phases. Fortunately, there has been considerable effort expended on this topic (Berner 1992, Lothenbach & Winnefeld 2006, Lothenbach & Gruskovnjak 2007, Matschei, Lothenbach & Glasser 2007). The themodynamic data determine the type and quantity of mineral phases dissolved or precipitated.

It is important to remember that thermodynamic data differ from kinetic data. The thermodynamic data will yield mineral composition at equilibrium. Kinetic coefficients determine the time required before the system reaches equilibrium. Few, if any, kinetic data exist for mineral phases relevant to cementitious systems. Over very long time scales, performance will be controlled by the properties of the very low solubility minerals, which are the minerals that will most likely have the slowest reaction kinetics.

4.2 MICROSTRUCTURAL PROPERTIES

Upon mixing with water, the cementitious constituents react to form the hydration products. The system is initially a colloidal suspension, and the hydrated reaction products consume more volume than the reactants, and begin filling the inter-particle space initially filled with

water. The solid grows through a combination of topo-chemical reactions and solution precipitation.

When a sufficient inter-connected network of solids exits, the paste will have mechanically "set", thereby supporting a pre-determined amount of shear stress. Continued hydration further fills in the void space with reaction products, thereby increasing the load carrying capacity, quantified in practice by the compressive strength. Not only is the total pore volume decreasing over time, the tortuosity of the pore space is simultaneously increasing; the tortuosity is a dimensionless number that represents the ratio of the characteristic path length through the pore space to the length of the specimen (a number that is greater than or equal to one).

The hydration process continues, conceptually, forever. Practically, however, most of the hydration has completed after one year. For modeling barrier performance over 100 to 1000 years of service, the hydration state at one year may be a practical initial condition, although changes in the environment or the microstructure could induce further hydration to occur. At this point, the key pieces of information for a performance assessment would be the types and quantity of mineral phases present, the total porosity remaining, and the relevant transport parameters: diffusivity, permeability, etc., which are sensitive functions of microstructure.

4.2.1 Porosity/Saturation

There are two types of porosity present in hydrated porous systems: water-filled porosity and air-filled porosity. The water filled porosity is further divided between C-S-H gel porosity, and capillary porosity. Hydration consumes water faster than the rate of hydration product formation. This chemical shrinkage results in cavitation and gas-filled pore space. Therefore, these systems are not completely saturated. Under sealed conditions, there is insufficient water for complete hydration for systems having a water:cement (mass) ratio less than approximately 0.38 because all capillary and gel pore water is consumed (Taylor 1997). Below a water:cement (mass) ratio of approximately 0.44, there is insufficient water at complete hydration to fill the gel pores (capillary pores empty), and a state of self-desiccation is achieved (Taylor 1997).

The capillary porosity ϕ_c of portland cement pastes can be approximated by a function of the degree of hydration α and the water:cement (mass) ratio β as shown in Equation 1:

$$\phi_c = 1 - \frac{1 + 1.16\alpha}{1 + 3.2\beta} \tag{1}$$

As an example, a 0.45 water:cement (mass) ratio has an initial capillary porosity of 0.59, and a capillary porosity of 0.11 at complete hydration. For most cementitious systems, the capillary porosity decreases by less than an order of magnitude over the course of hydration.

In addition to the capillary porosity, the C-S-H gel is composed of approximately 28 % porosity (Taylor 1997). Although this porosity is composed of much smaller pores than capillary pores, the C-S-H gel pores can contain water. This water can be removed at very low relative humidity, so it is able to exchange with capillary water. Moreover, the water-filled gel porosity can contribute to overall transport, but the gel pore relative transport coefficient[7] is orders of magnitude smaller than the corresponding capillary pore space transport coefficient.

Another factor to consider when characterizing porosity is the connectedness of the pore space. If there is sufficient capillary porosity that the capillary pores are connected across a sample, these interconnected capillary pores will likely dominate the rate of transport (assuming the samples is free of fractures or other macro defects). If the capillary porosity is below a critical volume fraction, the capillary pores will no longer be connected across the sample. Instead, transport through the sample must pass through both capillary pores and C-S-H gel pores.

4.2.2 Pore Size Distribution

Very little quantitative data exist on the pore size distribution in hydrated cementitious systems. Because the hydration products are continually filling in the water-filled pore space, the pore size distribution must shift toward smaller pores as hydration continues. The currently available microstructural computer models are incapable of resolving the pore network at a sufficient detail to fully characterize the pore size distribution down to the length scale of C-S-H pores.

The most direct experimental technique for characterizing the pore size distribution is mercury intrusion porosimetry (MIP). This technique forces a non wetting liquid into pore space at very high pressure into a dried specimen. The resulting data for the volume of liquid intruded as a function of pressure have to be corrected for physical parameters such as the contact angle between the fluid and the microstructure. Moreover, pore constrictions mean that the intruded volume indicates the volume of pore space accessible via a minimum pore throat, not the pore size distribution. Instead, MIP can be used to characterize the largest pore diameter that percolates the microstructure (Katz &Thompson 1987). As discussed below, this critical pore throat diameter can be used to estimate the hydraulic permeability.

4.2.3 Tortuosity

The tortuosity can be characterized qualitatively as the ratio of the path length through the pore space of a material, divided by the macroscopic length of the material. As more twists and turns are needed to pass through the pore space, the tortuosity increases. As additional solids precipitate, closing off pores, the tortuosity increases further. Therefore, tortuosity is a non-trivial function of the porosity and the pore size distribution and sometimes the specific transport mechanism considered (e.g. diffusion through a liquid vs. molecular diffusion

[7] Rate of diffusive transport through the gel pores, relative to diffusive transport through water.

through air). Moreover, there is no theoretical approach to this relationship, so it must be approximated with empirical relationships.

The relationship between porosity and tortuosity depends, in part, on how the material is formed. A relationship developed for sandstone does not apply to hydrated cement pastes because sandstone is formed from a cementing process, and the hydrated cement paste is a combination of cementing (prior to set) and diffusion limited aggregation (DLA). It is the DLA process that forms the portion of the microstructure that has the greatest impact on transport.

Given that the pore space is subdivided between liquid-filled and gas-filled, the tortuosity should likewise be subdivided. Therefore, there is a tortuosity for the liquid-filled space and a tortuosity for the gas-filled space. These are important concepts when the environment is not saturated with water vapor.

4.3 TRANSPORT PROPERTIES

From a performance assessment modeling perspective, microstructural changes via dissolution and/or precipitation lead to commensurate changes in transport coefficients. The two transport coefficients most relevant to cementitious barrier degradation are diffusivity and permeability.

4.3.1 Formation Factor

Diffusion is the primary transport mechanism in the absence of a hydraulic pressure gradient. Ionic diffusion occurs through the connected water-filled pore space, and vapor diffusion occurs through both the water-filled and vapor-filled pore space.

Diffusion can be described within the pore space (pore space diffusivity), or across a porous material (bulk diffusivity). The pore solution has an electrical conductivity σ_p, and the bulk material (saturated with the same solution) has electrical conductivity σ_b. The ratio of these two quantities can be used to approximate the formation factor F (Collins 1961):

$$F = \frac{\sigma_p}{\sigma_b} \tag{2}$$

As defined, the formation factor is a quantity having a value greater than or equal to one because the solid comprising the bulk material is assumed to be an electrical insulator. The formation factor can also be related to the porosity ϕ and the tortuosity τ:

$$F = \frac{\tau}{\phi} \tag{3}$$

n.b.: the definition of tortuosity can vary among authors, with some authors defining tortuosity as the inverse of the quantity used here.

The formation factor is a property of the solid microstructure, and does not depend on the composition of the pore solution. The ratio of the pore solution and bulk conductivities have a one-to-one relationship to the diffusion coefficient of an ion in the pore solution and the bulk diffusion coefficient. Therefore, one could use the formation factor to estimate the bulk diffusion coefficient using the diffusion coefficient of the species in the pore solution. This quantity, however, can only be estimated after the pore solution composition has been established.

Alternatively, the limiting ionic self-diffusion[8] coefficient D_i° (IUPAC 1976) is the diffusion coefficient of an ion in water in the limit that total concentration of all ions is zero (Harned & Owen 1958). Self-diffusion coefficients for different species can be found in reference books (Mills & Lobo 1989). Within an inert porous microstructure saturated with a very dilute pore solution and having formation factor F, the apparent bulk diffusivity D_i (Snyder 2001) can be estimated from the formation factor:

$$D_i = \frac{D_i^\circ}{F} \tag{4}$$

This is not a complete description of diffusion in cementitious materials because pore solution speciation, ion exchange, and (topo-) chemical reactions can alter the apparent diffusivity of an ionic species within the pore solution (Samson et al. 2005).

4.3.2 Permeability

Permeability is a more complex function of changes in the microstructure than diffusivity. Not only does it depend upon changes in the porosity and tortuosity, it (most importantly) depends upon the pore size distribution. Given that the permeability of hardened portland cement pastes can vary from 10^{-20} m^2 to 10^{-16} m^2, the relevant length scale that characterizes permeability is on the order of tens to hundreds of nanometers. Presently, there are no viable micro/nano-structure computer models for predicting the permeability of a hydrated cement paste based on an analysis of the modeled microstructure.

In addition, the bulk permeability of a composite element containing aggregates depends upon the permeability of the hydrated cementitious binder in both the bulk pore space and near the aggregate surfaces. As the aggregate volume increases, the higher permeability regions of the paste near aggregate surfaces begin to overlap. Above a critical aggregate volume, these regions can percolate the system, thereby greatly increasing the bulk permeability of the element (Winslow et al. 1994). This phenomenon occurs over the length scale of tens of millimeters.

[8] Molecular diffusion coefficient

For structures subjected to hydraulic pressure gradient, transport of ionic species is dictated by permeation. Under these conditions, the assumption is that the ions move with the pore solution. The pore solution volume averaged velocity is calculated from the D'Arcy flux $\boldsymbol{q}$:

$$\boldsymbol{q} = \frac{-k}{\eta}\nabla P \tag{5}$$

where k is the intrinsic permeability, η is the dynamic fluid viscosity, and ∇P is the fluid pressure gradient. The pore solution velocity $\boldsymbol{v}$ (tracer velocity) is faster than the flux by a factor of the porosity ϕ:

$$\boldsymbol{v} = \frac{\boldsymbol{q}}{\phi} \tag{6}$$

The Katz-Thompson (Katz & Thompson 1986, Katz & Thompson 1987) estimation for permeability k is proportional to the ratio of the square of a critical pore size diameter d_c to the formation factor F (dimensionless quantity):

$$k = \frac{c\, d_c^2}{F} \tag{7}$$

The constant of proportionality c varies, depending upon the particular microstructural formation mechanism, but is typically on the order of 10^1 to 10^2 (Garboczi 1990). The critical pore size diameter d_c is analogous to the diameter of the largest sphere that can pass through the pores.

Using the Katz-Thompson relationship in Eq. 7, one can see how the discontinuity of the capillary pores can have a dramatic effect on permeability. If the capillary pores are connected (percolate the system), the critical pore diameter would be on the order of 10^{-6} m. If the capillary pores no longer percolate the system (i.e., sufficient hydration at a low enough water:cement mass ratio), the critical pore diameter would have to be limited to that for the C-S-H, which would be on the order of 10^{-8} m. Given that permeability is proportional to $d_c^{\,2}$, the ratio of permeabilities for connected vs. disconnected capillary pores would be on the order of 10^4. Similarly, if leaching occurs in a system that initial has disconnected pores, at the point where capillary pores percolate the system, the permeability would increase dramatically.

4.4 MICROSTRUCTURAL EVOLUTION DURING DEGRADATION

There are two approaches to estimating the microstructural evolution during degradation. The first is to use empirical relationships between changes in porosity (through dissolution and precipitation) and changes in transport coefficients. The second approach attempts to first estimate the microstructural changes that occur, and then use this information to predict the resulting changes in the transport coefficients.

The first approach has the advantage of expediency, but requires sufficient measurement to ensure data over the relevant parameter space. The empirical relationships were developed using data for specific mixtures under specific conditions. Therefore, the data are only applicable to similar systems under similar conditions. Given enough data over a sufficient parameter space, one can begin applying the empirical relationships over a broad set of conditions. Applying the relationships to systems (materials + exposure) outside the parameter space leads to uncertainties that may be difficult to quantify.

The second approach has the advantage of being better able to adapt to new materials and exposure conditions. Once the microstructural model and the estimation of transport parameters (e.g., porosity, formation factor, etc.) have been validated for the materials and degradation mechanisms encountered, the approach can more easily adapt to new materials and exposure conditions. If the microstructural model is based on physical principles, once these are validated, the model applies wherever the same principles apply. Moreover, one does not need to have data for simultaneous degradation mechanisms (e.g., leaching and chloride diffusion), as these are simply manifestations of the chemical and physical principles that have been validated. Therefore, a microstructure-based degradation model can more reliably predict the performance of new materials in complex (varying in time or multiple mechanisms) environments for which there are no experimental data.

The challenge of a microstructure-based degradation model is predicting permeability. Because the permeability depends upon the details of pore sizes on the order of the critical pore diameter d_c, the microstructural model must somehow accurately resolve the pores at this scale. This is a particularly challenging requirement for a model, especially if the model is to perform calculations within a reasonable time limit.

4.4.1 Transport Properties

The evolution of transport properties during degradation is similar to the evolution of transport properties during hydration. Dissolution and precipitation of mineral phases change the porosity, the pore size distribution, and the pore connectivity. If the change in volume of mineral phases is small enough, and those mineral phases do not contribute directly to the critical pore diameter, both the diffusivity and the permeability will (roughly) vary inversely to changes in the porosity.

As the volume change increases, however, the tortuosity and critical pore diameter will change. Estimating the diffusivity and permeability will require either a microstructural model, or empirical relations based on previous experimentation. The same microstructural model used to predict the transport properties of the hydrated system would be applicable to changes in the microstructure due to degradation.

In the absence of microstructural information, changes in formation factor can be approximated by empirical power-law relationships (Grathwohl 1998). One possible expression is based Archie's law (Archie 1942) relating formation factor to porosity ϕ:

$$\Gamma = \phi^m \quad (8)$$

The exponent m is the material cementation exponent. This is a purely empirical relationship, and must be validated from a database of

When coupled to a microstructural model, however, the transport coefficients can be calculated directly. The formation factor (for diffusivity) can be calculated from the relative electrical conductivity of the pore space. The permeability can be calculated from the flow of fluid through the pore space due to a pressure difference across the microstructure.

5.0 SUMMARY

The mineralogical and microstructural changes that occur during hydration and reaction are numerous and complex. Treating the hydration and the degradation reactions on a similar basis, however, simplifies the problem to enumerating the relevant reactions, determining mineral phase dissolution and/or precipitation to achieve chemical equilibrium, and modifying the porosity and transport properties accordingly using a microstructure model. The accuracy of this approach depends upon a comprehensive characterization of the starting material and the environment, and upon comprehensive thermodynamic and kinetic data for the reactions.

The approach borrows from geochemical modeling, and is based on a strong foundation in thermodynamics. Moreover, the parameters have physical meaning and can be measured independently in the laboratory. As a result, the approach uses a minimum of empirical coefficients.

Although considerable information and data exist for the majority of reactions relevant to cementitious systems, additional information is needed for specific components of this approach. Applications involving waste isolation may occur at elevated temperatures. Additional work is needed to obtain missing data on the temperature dependence of the thermodynamic parameters of relevant mineral phases.

For very long term performance prediction, a combination of kinetic experiments and studies of natural/ancient analogs may be needed. The properties of the system after a thousand or more years will depend upon the mineral phases present. These phases may arise after re-crystallization of existing crystalline phases, or the crystallization of the amorphous calcium silicate hydrate gel. Data are needed to establish the kinetics of the crystallization reactions, and the resulting phases. Estimates of the very long-term mineral phase composition will then allow researchers to study the properties of these crystalline phases, and the kinetics data will be used to estimate when these properties will occur.

6.0 REFERENCES

Archie, GE 1942, 'The electrical resistivity log as an aid in determining some reservoir characteristics,' *Transactions of the AIME*, vol. 146, pp. 54-62.

ASTM 2005a, 'ASTM C 150: Standard Specification for Portland Cement', ASTM International, West Conshohocken, PA.

ASTM 2005b, 'ASTM C 618: Standard Specification for Coal Fly Ash and Raw or Calcined Natural Pozzolan for Use in Concrete', ASTM International, West Conshohocken, PA.

ASTM 2005c, 'ASTM C 1240: Standard Specification for Silica Fume Used in Cementitious Mixtures', ASTM International, West Conshohocken, PA.

ASTM 2006a, 'ASTM C 989: Standard Specification for Ground Granulated Blast-Furnace Slag for Use in Concrete and Mortars', ASTM International, West Conshohocken, PA.

ASTM 2006b, 'ASTM C 1365: Standard Test Method for Determination of the Proportion of Phases in Portland Cement and Portland-Cement Clinker Using X-Ray Powder Diffraction Analysis', ASTM International, West Conshohocken, PA.

Bakharev, T, Sanjayan, JG & Cheng, Y-B 2000, 'Effect of admixtures on properties of alkali-activated slag concrete', *Cement and Concrete Research*, vol. 30, pp. 1367-1374.

Bao, Y, Grutzeck, MW & Jantzen, CM 2005, 'Preparation and properties of hydroceramic waste forms made with simulated Hanford low-activity waste', *Journal of the American Ceramic Society*, vol. 88, pp. 3287-3302.

Barneyback, RS & Diamond, S 1981, 'Expression and analysis of pore fluids of hardened cement pastes and mortars,' *Cement and Concrete Research*, vol. 11, pp. 383-394.

Bentz, D.P. 1997, "Three-Dimensional Computer Simulation of Portland Cement Hydration and Microstructure Development", *Journal of the American Ceramic Society*, vol. 80, no**.** 1, pp. 3-21.

Berner, UR 1992, 'Thermodynamic modelling of cement degradation: Impact of redox conditions on radionuclide release', *Cement and Concrete Research*, vol. 22, pp. 465-475.

Bogue, RH 1929, 'Calculation of the compounds in portland cement', *Industrial & Engineering Chemistry Analytical Edition*, vol. 1, pp. 192-197.

Bogue, RH 1955, 'The Chemistry of Portland Cement', Reinhold Publishing Corporation, New York.

Bradford, A, Esh, D, Ridge, A, Thaggard, M, Whited, R, Treby, S, Flanders, S & Camper LW 2005, 'U.S. Nulcear Regulatory Commission Technical Evaluation Report for the U.S. Department of Energy Savannah River Site Draft Section 3116 Waste Determination for Salt Waste Disposal', *Technical Report*, U.S. Nuclear Regulatory Commission, *viii* + 106 pp.

Brough, AR, Katz, A, Bakharev, T, Sun, G-K, Kirkpatrick, RJ, Struble, LJ & Young, JF 1995, 'Microstructural aspects of zeolite formation in alkali activated cements containing high levels of fly ash,' *Proceedings of the Materials Research Society*, Vol. 370, pp. 199-208.

Buck, AD, Burkes, JP & Poole, TS 1985, 'Thermal stability of certain hydrated phases in systems made using portland cement', ADA160443 (Defense Technical Information Center OAI-PMH Repository).

Collins, RE 1961, *Flow of Fluids Through Porous Materials*, Reinhold Publishing.

Cook, JR, Wilhite, EL, Hiergesell, RA & Flach, GA 2005, 'Special Analysis: Revsion of the Saltstone Vault 4 Disposal Limits,' WSRC-TR-2005-00074, Westinghouse Savannah River Company, Aiken, South Carolina.

Cook, JR & Fowler, JR 1992, 'Radiological Performance Assessment for the Z-Area Saltstone Disposal Facility,' WSRC-RP-92-1360, Rev. 0, Westinghouse Savannah River Company, Aiken, South Carolina.

Crammond, NJ 2003, 'The thaumasite form of sulfate attack in the UK', *Cement and Concrete Composites*, vol. 25, pp. 809-818.

Garboczi, EJ 1990, 'Permeability, diffusivity, and microstructural parameters – A critical review', *Cement and Concrete Research*, vol. 20, pp. 591-601.

Gartner, EM, Tang, FJ, & Weis, SJ 1985, 'Saturation factors for calcium hydroxide and calcium sulfates in fresh portland cement pastes,' *Journal of the American Ceramic Society*, vol. 68, pp. 667-673.

Goldschmidt, A 1982, 'About the hydration theory and the composition of the liquid phase of portland cement,' *Cement and Concrete Research*, vol. 12, pp. 743-746.

Grathwohl, P 1998, *Diffusion in Natural Porous Media: Contaminent Transport, Sorption/Desorption and Dissolution Kinetics*, Springer.

Gruskovnjak, A, Lothenbach, B, Holzer, L, Figi, R & Winnefeld, F 2006, 'Hydration of alkali-activated slag: Comparison with ordinary portland cement', *Advances in Cement Research*, vol. 18, pp. 119-128.

Gruskovnjak, A, Lothenbach, B, Winnefeld, F, Figi, R, Ko, S-C, Adler, M & Mäder, U 2008, 'Hydration mechanisms of super sulphated slag cement', *Cement and Concrete Research*, vol. 38, pp. 983-992.

Harned HS. & Owen BB 1958, *The Physical Chemistry of Electrolytic Solutions*, Reinhold Publishing Corporation, New York.

Hong S.-Y. & Glasser, FP 1999, 'Alkali binding in cement pastes: Part I. The C-S-H phase,' *Cement and Concrete Research*, vol. 29, pp. 1893-1903.

Hong S.-Y. & Glasser, FP 2002, 'Alkali sorption by C-S-H and C-A-S-H: Part 2. Role of alumina,' *Cement and Concrete Research*, vol. 32, pp. 1101-1111.

Huang, C-Y & Feldman, RF 1985a, 'Influence of silica fume on the microstructural development in cement mortars', *Cement and Concrete Research*, vol. 15, pp. 285-294.

Huang, C-Y & Feldman, RF 1985b, 'Hydration reactions in portland cement-silica fume blends', *Cement and Concrete Research*, vol. 15, pp. 585-592.

IUPAC 1976, "Manual of Symbols and Terminology for Physicochemical Quantities and Units - Appendix II. Definitions, Terminology and Symbols in Colloid and Surface Chemistry. Part II: Heterogeneous Catalysis", *Pure and Applied Chemistry*, vol. 46, pp. 71-90.

Jappy, TG and Glasser, FP 1991, 'Synthesis and stability of silica-substituted hydrogarnet $Ca_3Al_2Si_{3-x}O_{12-4x}(OH)_{4x}$', *Advances in Cement Research*, vol. 4, pp. 1-8.

Jiang W, Silsbee, MR & Roy, DM 1997, 'Alkali activation reaction mechanisms and it influences on microstructure of slag cement', *Proceedings of the 10th International Congress on the Chemistry of Cement (Göteborg)*, vol. 3, p. 3ii100 (9 pp.).

Jull, SP & Lees, TP 1990, 'Studies of historic concrete,' CEC Technical Report No. 12972, CEC, Brussels.

Katz, A, Brough, AR, Kirkpatrick, RJ, Struble, LJ & Young, JF 2000, 'Effect of solution concentration on the properties of a cementitious grout wasteform for low-level nuclear waste,' *Nuclear Technology*, vol. 129, pp. 236-245.

Katz, AJ & Thompson, AH 1986, 'Quantitative prediction of permeability in porous rocks', *Physical Review B*, vol. 34, pp. 8179-8181.

Katz, AJ & Thompson, AH 1987, 'Prediction of rock electrical conductivity from mercury injection measurements', *Journal of Geophysical Research*, vol. 92, pp. 599-607.

Lichtner, PC, Steefel, CI & Oelkers, EH (Editors) 1996, *Reactive Transport in Porous Media*, Reviews in Mineralogy (Volume 34), Mineralogical Society of America, Washington, D.C.

Longuet, P, Burglen, L & Zelwer, A 1973, '*La phase liquide du cement hydraté*' (in Fr.) *Revue des Matériaux de Construction*, vol. 676, pp. 35-41.

Lothenbach, B & Winnefeld, F 2006, 'Thermodynamic modelling of the hydration of Portland cement', *Cement and Concrete Research*, vol. 36, pp. 209-226.

Lothenbach, B & Gruskovnjak, A 2007, 'Hydration of alkali-activated slag: Thermodynamic modeling', *Advances in Cement Research*, vol. 19, pp. 81-92.

Matschei, T, Lothenbach, B & Glasser, FP 2007, 'Thermodynamic properties of Portland cement hydrates in the system CaO-Al_2O_3-SiO_2-$CaSO_4$-$CaCO_3$-H_2O', *Cement and Concrete Research*, vol. 37, pp. 1379-1410.

Michaux, M, Fletcher, P, & Vidick, B 1989, 'Evolution at early hydration times of the chemical composition of liquid phase of oil-well cement pastes with and without additives. Part I. Additive free cement pastes,' *Cement and Concrete Research*, vol. 19, pp. 443-456.

Mills R. & Lobo V.M.M. 1989, *Self-Diffusion in Electrolyte Solutions*, Elsevier, New York.

Mindess S & Young, JF 1981, *Concrete*, Prentice-Hall, Englewood Cliffs.

Parkhurst, DL & Appelo, CAJ 1999, 'User's guide to PHREEQC (Version 2)--a computer program for speciation, batch-reaction, one-dimensional transport, and inverse geochemical calculations', Report 99-4259 (U.S. Geological Survey) 312 p.

Paul, M & Glasser, FP 2000, 'Impact of prolonged warm (85 °C) moist cure on Portland cement paste', *Cement and Concrete Research*, vol. 30, pp. 1869-1877.

Petit, JC 1992, 'Natural analogues for the design and performance assessment of radioactive waste forms: A review', *Journal of Geochemical Exploration*, vol. 46, pp. 1-33.

Rassineux, F, Petit, JC, & Meunier, A 1989, 'Ancient analogues of modern cement: Calcium hydrosilicates in mortars and concretes from Gallo-Roman thermal baths of Western France,' *Journal of the American Ceramic Society*, vol. 72, pp. 1026-1032.

Regourd, M 1980, 'Structure and behavior of slag Portland cement hydrates', *Proceedings of the 7th International Congress on the Chemistry of Cement (Paris)*, vol. 1, pp. III-2 / 10-26.

Regourd, M 1986, 'Ciments spéciaux et ciments avec additions', *Proceedings of the 8th International Congress on the Chemistry of Cement (Brasil)*, vol. 1, pp. 199-227.

Richardson, IG & Groves, GW 1992, 'Microstructure and microanalysis of hardened cement pastes involving ground granulated blast-furnace slag', *Journal of Materials Science*, vol. 27, pp. 6204-6212.

Samson, E, Marchand J, Snyder, KA & Beaudoin, J 2005, 'Modeling ion and fluid transport in unsaturated cement systems in isothermal conditions', *Cement and Concrete Research*, vol. 35, pp. 141-153.

Scrivener, K.L. & Bishnoi, S. 2009, 'Microstructural model for portland cement paste', submitted to *Cement and Concrete Research*.

Scrivener, K.L. & Taylor, HFW 1993, 'Delayed ettringite formation: A microstructural and microanalytical study,' *Advances in Cement Research*, vol. 5, pp. 139-146.

Shehata, MH & Thomas, MDA 2002, 'Use of ternary blends containing silica fume and fly ash to suppress expansion due to alkali-silica reaction in concrete', *Cement and Concrete Research*, vol. 32, pp. 341-349.

van der Sloot, HA, Hoede, D, Rietra, RPJJ, Stenger, R, Lang, Th., Schneider, M, Spanka, G, Stoltenberg-Hansson, E & Lerat, A 2001, 'Environmental Criteria for Cement Based Products ECRICEM Phase I: Ordinary Portland Cements', ECN C-01-069.

Smolczyk, HG 1980, 'Slag structure and identification of slags', *Proceedings of the 7th International Congress on the Chemistry of Cement (Paris)*, vol. 1, pp. III-1 / 3-17.

Snyder, KA 2001, 'The relationship between the formation factor and the diffusion coefficient of porous materials saturated with concentrated electrolytes: Theoretical and experimental considerations', *Concrete Science and Engineering*, vol. 3, pp. 216-224.

Snyder, KA & Marchand, J 2001, 'Effect of speciation on the apparent diffusion coefficient in nonreactive porous systems', *Cement and Concrete Research*, vol. 31, pp. 1837-1845.s

Solem, JK & McCarthy, GJ 1992, 'Hydration reactions and ettringite formation in selected cementitious coal conversion by-products', *Materials Research Society Symposium Proceedings*, vol. 245, pp. 71-79.

Steadman, JA 1986, 'Archaeological concretes as analogues', *Proc. Second NAWG Meeting*, Interlaken, Switzerland, CEC Technical Report No. EUR 10671 EN, CEC Brussels, pp. 165-171.

Stutzman, PE 2009, 'Effects of analytical precision on Bogue calculations of potential cement composition', (to be submitted) *ASTM International*.

Taylor, HFW 1987, 'A method for predicting alkali ion concentrations in cement pore solutions,' *Advances in Cement Research*, vol. 1, pp. 5-17.

Taylor, HFW 1997, *Cement Chemistry*, (Second Edition), Thomas Telford, London.

Traetteberg, A 1978, 'Silica fume as a pozzolanic material', *Il Cemento*, vol. 75, no. 3, pp. 369-376.

Uchikawa, H 1986, 'Effect of blending components on hydration and structure formation', *Proceedings of the 8th International Congress on the Chemistry of Cement (Rio de Janeiro)*, vol. 1, pp. 249-280.

Wang, S-D & Scrivener, KL 1995, 'Hydration products of alkali activated slag cement', *Cement and Concrete Research*, vol. 25, pp. 561-571.

Winslow, DN, Cohen, MD, Bentz, DP, Snyder, KA & Garboczi, EJ 1994, 'Percolation and pore structure in mortars and concrete', *Cement and Concrete Research*, vol. 24, pp. 25-37.

Yuan, C-Z & Xin, L 1992, 'The selection of stimulation agents for alkali-slag cement', *Proceedings of the 9th International Congress on the Chemistry of Cement (New Delhi)*, vol. 3, pp. 305-311.